Nano Energy (2014) 6, 36–43

Available online at www.sciencedirect.com

ScienceDirect

journal homepage: www.elsevier.com/locate/nanoenergy

RAPID COMMUNICATION

A broadband and omnidirectional light-harvesting scheme employing nanospheres on Si solar cells

Guan-Jhong Lin[a,1], Hsin-Ping Wang[a,1], Der-Hsien Lien[a], Po-Han Fu[a], Hung-Chih Chang[a], Cheng-Han Ho[a], Chin-An Lin[a], Kun-Yu Lai[b], Jr-Hau He[a,c,*]

[a]Institute of Photonics and Optoelectronics, National Taiwan University, Taipei 10617, Taiwan
[b]Department of Optics and Photonics, National Central University, Chung-Li 320, Taiwan
[c]Department of Electrical Engineering, National Taiwan University, Taipei 10617, Taiwan

Received 23 January 2014; received in revised form 1 March 2014; accepted 3 March 2014
Available online 12 March 2014

KEYWORDS
Light harvesting;
Nanospheres;
Solar cells;
Omnidirectionality;
Scattering

Abstract
The optimized nanospheres (NSs) are simulated and then employed as light-harvesting nanostructures on Si solar cells (SCs). Uniformly distributed monolayers of NSs effectively suppress the reflection over the broadband region at the incident angles up to 85°, greatly improving the optical absorption of the SCs. The calculation results indicating significant reflection elimination and strong forward scattering agree with those obtained by experimental measurements, where the devices with NSs exhibit improved external quantum efficiencies by 13% at 800 nm and conversion efficiency by 21.6%. This simple, controllable and scalable fabrication of broadband and omnidirectional light-harvesting nanostructures is desired from the standpoint of practical applicability in SCs.

Introduction

Among the materials chosen for photovoltaic applications, Si is one of the most popular candidates due to its abundance on earth and well-developed processes [1]. Si-based solar cells currently take more than 70% in the solar power market [2]. Despite the dominant market share, commercially available Si solar cells still produce the energy conversion efficiencies well below those reported by laboratories or theoretical predictions [3]. It has been known that the high refractive index of Si makes 40% of the incident light wasted through surface reflection [4]. In order to tackle the problem, single- or

*Corresponding author. Tel.:+886 2 3366 9646.
E-mail address: jhhe@cc.ee.ntu.edu.tw (J.-H. He).
[1]These authors contributed equally to this work.

http://dx.doi.org/10.1016/j.nanoen.2014.03.004
2211-2855/

multi-layered antireflective coating (ARC) is the most widely used ARCs in the industry due to their simplicity and cost- and time-effective fabrication processes. However, single- or multi-layered ARC with various problems, such as poor adhesion, limited working wavelength range, and angel of incident light. Materials for layered ARCs need to be carefully selected with the proper refractive indices. A lack of materials with refractive indices close to the refractive index of air is a critical problem. Moreover, light propagated through layered ARCs is a plane electromagnetic wave without scattering, leading to straight propagation of the incident light through the medium; *i.e.*, the optical thickness is almost equal to the actual thickness. Many research groups have demonstrated that monocrystalline Si solar cells based on a variety of Si nanostructures not only mitigate the undesired surface reflectance significantly but also allow a radial distribution of p-n junction through a core-shell structure, which benefits the collections of photocarriers [5-8]. Unfortunately, most attempts using nanostructured monocrystalline Si have shown unsatisfactory results; even with the complicated processes, Si nanostructured solar cells have shown a low efficiency due to large shunting across the cells, nonconformal deposition of the metal contacts over high aspect-ratio Si nanostructures and excessive junction/surface recombination losses [9]. For example, a single coaxial Si nanorod solar cell with a conversion efficiency of 3.4% had been reported [10]. Si nanowire array-based solar cells with a conversion efficiency of 5% were achieved [11,12]. The monocrystalline Si solar cells with nanohole array geometry exhibits superior optical absorption ability and conversion efficiency as high as 9.51% [5].

For overcoming the drawback created by nanostructuring monocrystalline Si solar cells mentioned above, numerous nanostructures obtained with other material systems directly grown on Si solar cells have been reported as the ideal light harvesting materials [7,13,14]. For example, the performance of monocrystalline Si solar cells can be substantially improved by integration of metal nanoparticles [13]. They not only provide an efficient radial charge-carrier collection, but also introduce plasmonic effects in addition to scattering effect to scatter incident light into a distribution of angles, increasing the path length of the light within the absorbing layer [15-19]. However, the metal nanoparticles inevitably cause light reflection. For the optimized parameters, metal nanoparticles still absorb up to 60% of the sunlight in the resonant region, which greatly degrade the applicability of metal nanoparticles than dielectric ones [20]. ZnO honeycomb sub-wavelength structure using nanosphere (NS) lithography technology exhibiting broadband antireflection properties shows substantially improved conversion efficiency of Si solar cells [21]. It has been reported that antireflective nanostructures exhibit many characteristics superior to those of their $\lambda/4$ counterparts, such as broadband working ranges, omnidirectionality, and independent polarizations [22-24].

Periodic nanostructures have been fabricated with a variety of techniques such as anodic aluminum oxide template [25], and electrochemical etching technique [8]. Polystyrene (PS) NS has been demonstrated to be useful for a variety of the applications due to its simplicity, scalability, and low cost [26-28].

In this study, for optimizing the dimension of NS structures, we employ a simulation work, indicating that the NS array with 450 nm in diameter reduces reflection and facilitates transmission more efficiently than the other sizes in the 600-950 nm regions, where Si has the highest photoelectric conversion efficiency. NS structure with 450 nm in diameter demonstrates excellent omnidirectional and broadband AR properties from the experimental and simulated data. PS NSs significantly suppress the surface reflection at the incident angles up to 85° over the broadband region. Close-packed NSs act as an intermediate layer with the graded effective refractive index between those of air and Si. The graded refractive index avoids the abrupt transition from air to Si and thus facilitates light traveling across the interface, overcoming a lack of materials with refractive indices close to the refractive index of air. Moreover, light propagated through NS structures (*i.e.*, submicron structures) deviates from rectilinear propagation and start to scattering, which can further enhance the effective optical thickness and the light absorption of devices. The absorption improvement is supported by the experiment results of external quantum efficiencies (EQEs) and conversion efficiencies under the air mass 1.5 global (AM 1.5 G) illumination and the simulation results. The devices with PS NSs exhibit improved EQEs by up to 13% at 800 nm, thus enhancing the conversion efficiency by up to 21.6%. The simple yet effective scheme using broadband and omnidirectional light-harvesting NSs is applicable not only to Si solar cells, but also to many other commercial photovoltaic devices.

Experimental section

Si solar cells used here were fabricated with single crystalline p-type (100) Si substrates (ρ=8-12 Ω cm). The substrates were first cleaned in acetone, followed by a HF dip to remove the native oxide from the surfaces. The concentration of HF for all the samples was 4.6 M. The n-emitter layer was formed by phosphorus doping at p-type substrates. The source of phosphorus doping was the P_2O_5 solution (P509). The P_2O_5 solution was spin-coated on the p-type substrate and annealed at 950 °C for 20 min. After annealing, the surface thermal oxide was removed by HF. The front electrode Ti/Ag and the back electrode Al were deposited by electron beam evaporation.

The solution of colloidal PS NSs diluted in deionized water was then coated on the surface of Si solar cells with a volume-controlled pipette. The devices were held in an incubator at 50 °C and 87.5% relative humidity for 2 h, and a close-packed hexagonal PS monolayer was formed upon drying solution. The PS monolayer was uniformly distributed on the device surface, and the period (center-to-center distance) of the close-packed NSs is 450 nm.

Results and discussion

Before fabricating the monocrystalline Si solar cells with the PS NS arrays, we employ a simulation work for optimizing the parameters of NSs. Based on the information provided by the simulation, we could predict and optimize the dimension of NS structures. We employed the rigorous coupled-wave analysis (RCWA) to gain the insight of size-dependent optical behavior of the NSs, which provides us

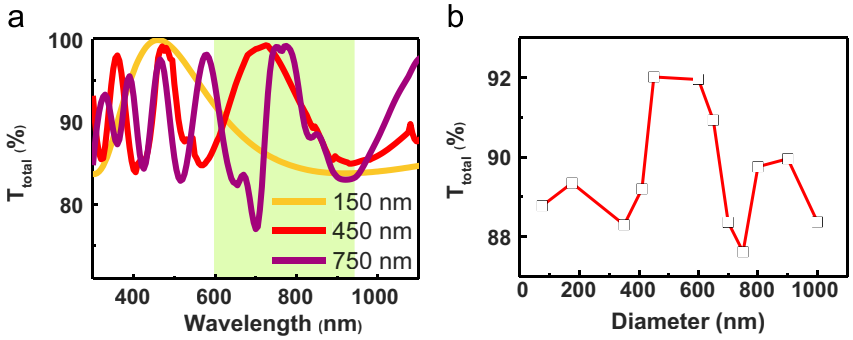

Fig. 1 (a) Total transmittance of PS NS structures with 150, 450 and 750 nm in diameter simulated by RCWA analysis with TE-polarized waves. (b) The average value of the total transmittance at the region of 600–950 nm.

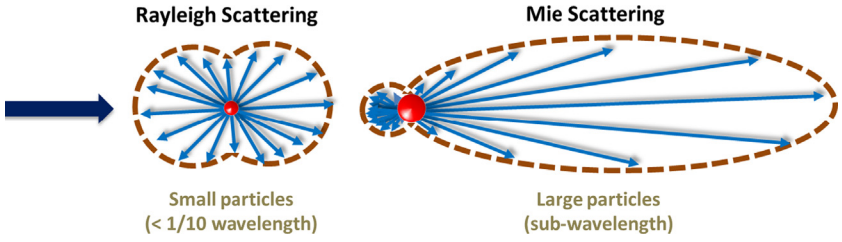

Fig. 2 Illustration of Rayleigh and Mie scattering.

the criteria to design the NSs. It was done by comparing the transmission spectrum of NSs with different diameters; for example, three kinds of feature sizes of PS NS structures, *i.e.*, diameters (d)=150, 450, and 750 nm, are shown in Fig. 1a. Note that the transmittance is the total transmittance (T_{total}) and the oscillation of transmittance is because of the multiple scattering beams interference caused by ordered hexagonal closed-packed arrangement, *i.e.*, Fabry-Pérot oscillations effect. It is difficult to find the tendency from the figure due to the close value and oscillation in T_{total} of three structures; hence as shown in Fig. 1b, we average the calculated T_{total} with a variety of NS diameters in the wavelength range of 600–950 nm, where the Si solar cells employed in this study have the highest photoelectric conversion efficiency. The transmittance shows an apparent peak at the NS with d=450 nm, where a decrease of T_{total} at the d below 425 nm indicates a transition of scattering mechanism from Mie to Rayleigh (which will be discussed in detail later), and the T_{total} decrease at the d higher than 650 nm can be attributed to the higher NS absorption due to larger size of NSs. This means that the NS structure with d=450 nm reduces reflection and facilitates transmission more efficiently than the others, exhibiting a superior light-harvesting performance for Si absorption. Accordingly, we choose the NS with d=450 nm to investigate the light-harvesting effect for Si solar cells.

Previously, NSs with the sizes ranging from 0 to 50 nm have been simulated [20], while NSs with larger size (from 150 to 1000 nm) were employed in our simulation work. The difference in nanoparticle size results in different light scattering behaviors, which could be categorized in two frameworks according to nanoparticle dimensions. When the scattering centers are much smaller than incident wavelength ($<$ 1/10 wavelength), *e.g.*, molecules or tiny particles, Rayleigh scattering is predominant. For Rayleigh scattering, the scattering intensity is a function of wavelength (λ^{-4} for particles and λ^{-3} for rods), and forward and reverse intensities are of the same magnitude [29,30], as shown in Fig. 2. On the other hand, Mie scattering occurs when the size of the scatter centers are comparable with the incident wavelength, where the forward scattering intensity is greater than that of the reverse scattering (Fig. 2) [15,30,31]. In the simulation work presented by Akimov et al., the Rayleigh scattering is the dominant mechanism for the solar absorption due to the small size of nanoparticles (nanoscale structure). In contrast, our NS structure with 450 nm in diameter (sub-wavelength structure) is more likely to obey the Mie theory [32–34]. This information tells us that, for maximizing the optical enhancement *via* applying NSs on optoelectronic devices, NSs should be appropriately chosen due to size-dependent scattering behaviors. For example, the small NSs (nanoscale structure, which causes Rayleigh scattering) are proposed to be the effective scattering centers capable of omnidirectional internal scattering, so that it should be applied within the nanowire arrays or embedding in the active layer [35–37]. The small NSs spherical scatter the incoming light to enhance the active region absorption. Liao et al. embedded different concentration of inorganic nanoparticles in hybrid solar cells. The distinctive inorganic nanoparticles-tuned nanostructures are thermally stable and exhibit significantly enhanced electron mobility, short-circuit current density (Jsc), and photovoltaic device performance [37]. In our case, submicron NSs (submicron structure, which causes Mie scattering) are more suitable for depositing on the surface of optoelectronic devices due to the stronger forward scattering [38]. Fang et al. proposed a strategy for enhancing the efficiency of solar cells by arranging different sizes of nanoparticles [39]. The small-size (sub-50 nm in diameter) nanoparticles are constructed to an optical gradient

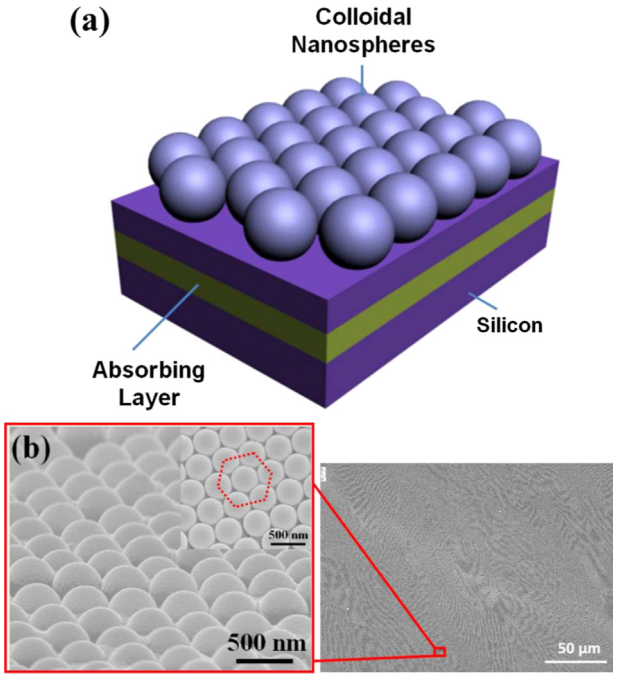

Fig. 3 (a) Schematic of Si solar cells with colloidal PS NSs. (b) 45°-tilted-view SEM image of colloidal PS NSs on Si solar cells (left). The inserted top-view SEM image in the left image shows the monolayer and HCP arrangement of colloidal PS NSs, indicated by a red-dashed line. Low-magnification top-view SEM image of colloidal PS NSs on Si solar cells (right).

nanoparticle stack to not only decrease reflectance, but also spherical scatter light. The large nanoparticles with sizes similar to the incident wavelength, exhibiting strong forward scattering, are applied to expand the acceptance angle of incident light for solar cells. Going forward, taking advantage of each scattering schemes to come up with creative designs appears to have the greatest potential for achieving high performance and cost-effective solar cells.

Fig. 3a presents the schematic of Si solar cell with colloidal PS NSs, and the 45°-tilted-view image of colloidal PS NSs recorded by a JEOL JSM-6500 field emission scanning electron microscope (SEM) is shown in Fig. 3b. The PS NSs are monolayer-thick and uniformly distributed over the device surface. As shown in the inset of Fig. 3b, the arrangement of NSs is hexagonal closed-packed (HCP) indicated by the red-dashed line, and the average diameter of the PS NSs is around 450 nm. The low-magnification SEM images show uniform distribution of PS NS arrays, demonstrating the feasibility for production. Due to the great uniformity, the strong interference fringes can be seen in the low-magnification SEM image.

AR characteristics of the PS NSs are investigated in Fig. 4a, where it shows the reflectance spectrum measured on two Si solar cells with different surface conditions: (i) bare surfaces (without any AR layers) and (ii) with the colloidal PS NSs. The spectra were obtained using a standard UV-vis spectrometer equipped with an integral sphere at the normal incident and the λ ranging from 400 nm to 800 nm. The suitability of PS NSs for the light-harvesting layer on solar cells is manifested by the fact that the surface reflection on the NSs is lower than that on the bare surface over the entire visible λ. Such a broadband light-harvesting property would not be attainable with conventional quarter-wavelength ARC. Compared with that on the bare surface, the reflectance on the colloidal PS NSs is mostly reduced in the λ range of 650–800 nm. The reflectance reduction is also observed in the range of 450–550 nm. At $\lambda \approx 580$ nm, a peak is noticed, which will be discussed later. The suppressed reflection on PS NSs can be related to several effects. In the short λ region, the feature size of NSs, such as the spacing between NSs, is resolved, which reduces the reflectance through the scattering of incident light. The induced scattering prolongs optical path within the nanostructure, and is expected to increase the probability of the incident light entering the device. In the long λ region, the features of PS NSs are less resolved and the reduction of reflectance can be explained by the effective medium theory [8]. Close-packed NSs act as an intermediate layer with the effective refractive index between those of air and Si. The intermediate refractive index avoids the abrupt transition from air to Si and thus facilitates light traveling across the interface.

The superior AR performances of PS NSs are supported by theoretical analyses. Fig. 4a also shows the simulated reflectance by RCWA performed on the bare surface and on the NSs. In the simulation, the λ-dependent refractive indices and extinction coefficients of PS NSs and Si are all considered [40]. It can be seen that the tendency of simulated curves generally agree with the measurement results. The slight difference between simulated and measured reflectance could be attributed to the imperfection of the colloidal PS NS structures and the misestimated doping concentration at the surface in the practical solar cells [41]. The reflectance peak at around 580 nm can be explained by the modified Bragg's law:

$$2\bar{n}d_g \sin\theta_i = m\lambda \tag{1}$$

where $\bar{n}$ is the average refractive index, m is the order of diffraction, θ_i is the angle of incidence, and d_g is the grating period [42]. Here, the incident light is approximately normal to the device surface, *i.e.*, $\sin\theta_i \approx 1$. For the HCP NSs, the d_g of PS NSs is estimated to be $\sqrt{3}D_s/2$ with D_s the diameter of a NS, which can be obtained in Fig. 3b. The $\bar{n}$ can be described by the following equation [41]:

$$\bar{n} = \sqrt{n_{sp}^2 f + n_{air}^2(1-f)} \tag{2}$$

where $f \approx 0.74$ is the filling ratio of the PS NSs, estimated using the SEM images and $n_{sp}=1.59$ and $n_{air}=1$ are the refractive indices of PS and air, respectively. According to above statements, as $m=2$, the peak at 580 nm is observed in Fig. 4. The results indicate that special care must be taken in the future to avoid Bragg reflections as designing the periodic NSs for efficient light harvesting.

In addition, for applying into a practical environment where the sunlight impinges the earth in various directions, the evaluation of reflectance over a wide range of incident angles is required, *i.e.*, the omnidirectional characterization. To investigate the effect of the colloidal PS NSs on the omnidirectionality of the Si solar cell, specular reflectance measurements, implemented on the polished Si wafer without and with the colloidal PS NSs under the detection angle

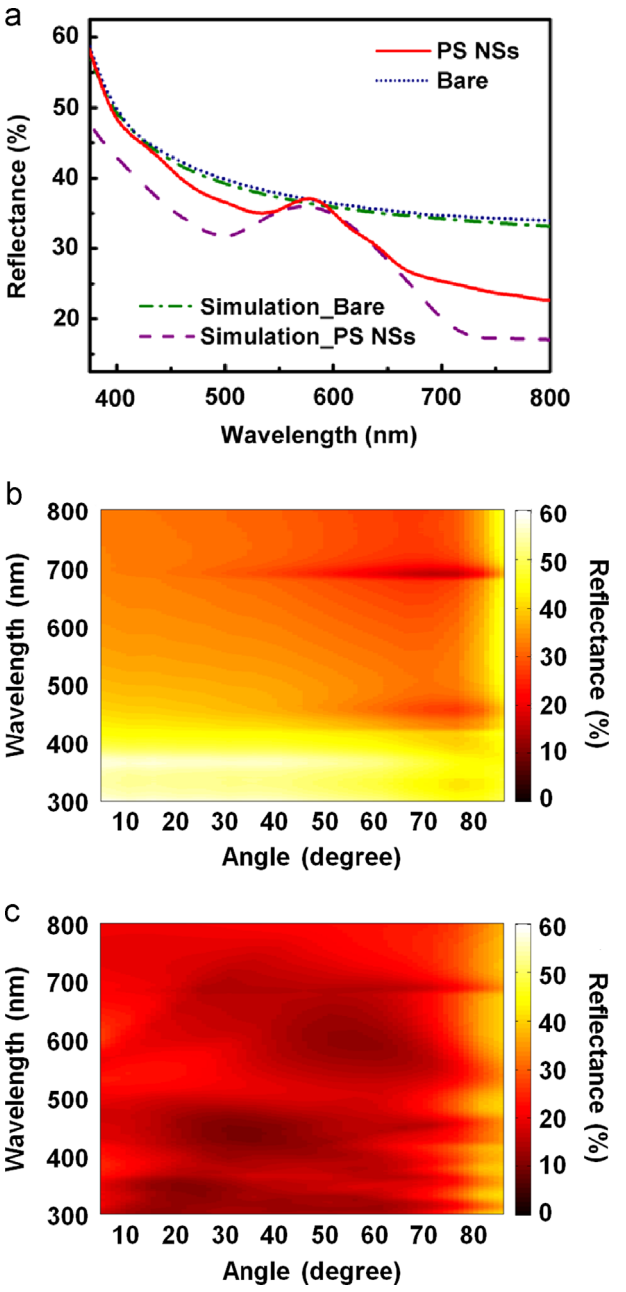

Fig. 4 (a) Reflectance spectra measured and simulated on the Si solar cells with different surface conditions, *i.e.*, bare and the colloidal PS NSs. Specular reflectance spectra with incident angles for polished Si wafers (b) without the colloidal PS NSs and (c) with the colloidal PS NSs. The incident angles are from 5° to 85° and the wavelengths are from 300 nm to 800 nm, and the detection angle is equivalent to the incident angle.

equivalent to the incident angle, are performed for the incident angle up to 85° and the wavelength up to 800 nm, as shown in Fig. 4b and c, respectively. As compared with the bare surface, it is observable that the reflectance of Si with PS NSs is significantly lower than that of Si without PS NSs over the whole incident angles, indicating that the colloidal PS NSs exhibit excellent omnidirectional light-harvesting characteristics and thus make the reflectance insensitive to incident angles. Therefore, as the light

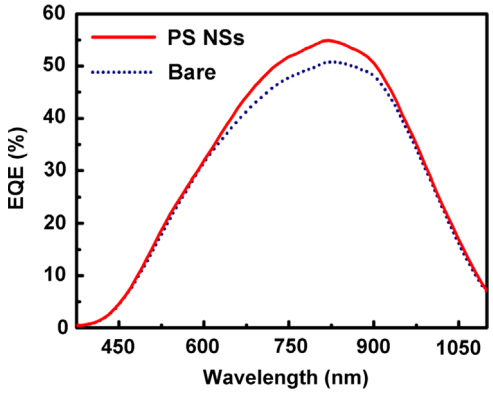

Fig. 5 EQE of the Si solar cells measured with the bare and colloidal PS NS surfaces.

reaches the surface of PS NSs, light will enter and be trapped within this layer, leading to additional photons into the absorbed layer and the enhancement of conversion efficiency.

The EQEs for the solar cells with and without the colloidal PS NSs are shown in Fig. 5. This measurement using Enli QE-R was carried out under the monochromatic illumination by a halogen lamp coupled to a monochromator. The enhanced EQEs are clearly observed in the λ ranging from 610 to 950 nm. At 800 nm, the maximum improvement of around 13% is obtained. As compared to the efficiency enhancement *via* surface plasmons using metal nanoparticles only at or near the plasmon resonance wavelengths, the efficiency of Si solar cells can be broadbandly improved due to the enhanced coupling of incident light into the device and scattering effects of PS NSs [13].

In addition to RCWA simulation, we also carried out finite-difference time-domain (FDTD) simulation aiming to reveal the distribution of electric fields across the boundaries of solar cells, through which the light harvesting effect of NSs and the absorption behaviors of the devices can be correlated. The FDTD analysis was performed on the solar cells with and without the NSs. In the simulation, steady-state values of the electric fields were calculated using 2D finite element software. The grid sizes are $\Delta x \times \Delta y = 5 \times 5\ \text{nm}^2$ in the space domain, and the time step for every calculation is 0.0099 fs. Boundaries in x and y directions are surrounded by the 0.5-μm perfectly matching layers to absorb the electromagnetic waves [43]. 800 nm at which noticeable EQE enhancement by the NSs is measured is chosen for the simulation of transmissions and reflections. Fig. 6a and b presents the time-averaged TE-polarized electric field intensity $|E_z|$ distributions within different surface conditions of solar cells at the incident λ of 800 nm. All of the displayed $|E_z|$ values are normalized to those of the excitation source, and the active region is indicated by the red-dashed lines. One can see that the NSs not only facilitate wave propagation into the device by the less abrupt interfaces, but also increase the lateral distribution of the fields by introducing light scattering on the surface. In Fig. 6c, normalized steady-state optical power integrated over the active region (denoted as P_T) is shown for the bare surface and the NSs with incident λ of 800 nm. The transmitted optical power is enhanced from 0.58 to 0.80 upon the application of NSs.

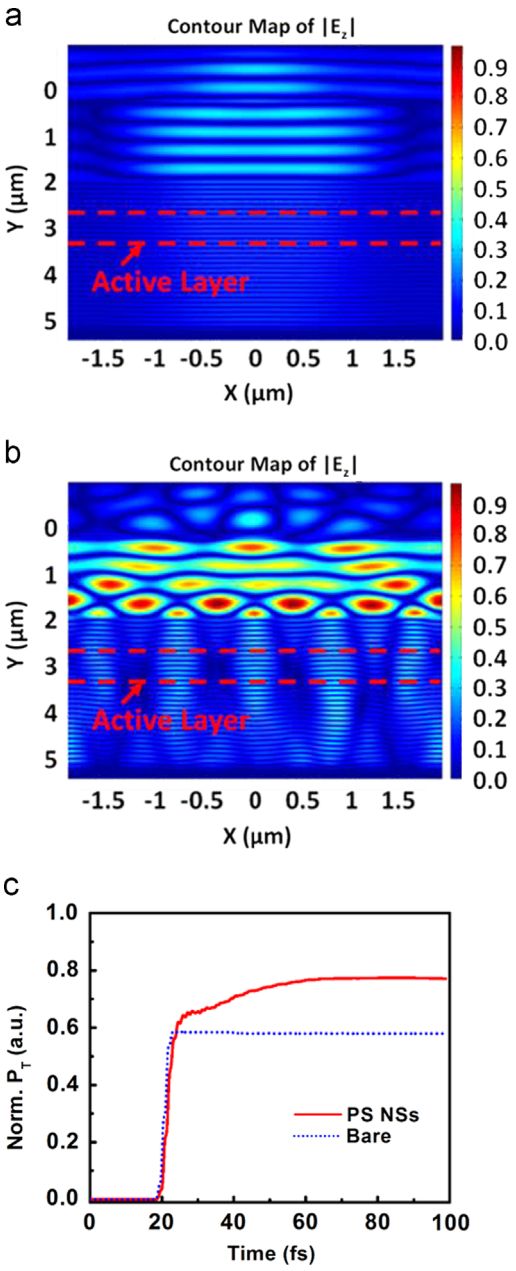

Fig. 6 Time-averaged and normalized TE electric field distribution at the incident wavelength of 800 nm simulated by FDTD analysis within the Si solar cells containing different surface conditions: (a) bare and (b) NSs. (c) Normalized optical power integrated over the active layer as a function of time on bare and NS surfaces with the incident wavelengths of 800 nm.

Fig. 7 represents the current density–voltage (*J*–*V*) curves of the solar cells measured under the illumination of AM 1.5 G solar simulator. Compared with the solar cell without NSs, the J_{sc} is increased from 27.4 mA/cm^2 to 28.2 mA/cm^2, indicating an enhanced solar absorption by the active layer. The enhanced J_{sc} results in the conversion efficiency improvement of the order of 21.6%. This result is consistent with those by FDTD simulation and EQE measurements. The photovoltaic performances are expected to be further enhanced as the periodic arrangement of PSs can be optimized such that the induced Bragg reflection occurs outside the λ range of device absorption.

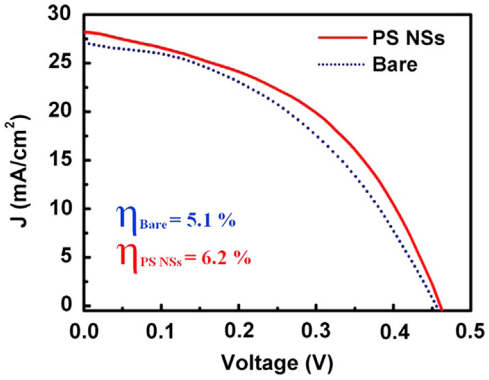

Fig. 7 *J*–*V* characteristics measured on the Si solar cells with bare and colloidal PS NSs surfaces.

Conclusion

In summary, a colloidal monolayer of PS NS arrays with 450 nm in diameter shows the superior light-harvesting characteristics for single crystalline Si solar cells by suppressing the surface reflection and enhancing forward scattering. The PS NS light-harvesting layer results in increased EQE peak at 800 nm by 13% and conversion efficiency by 21.6%. Theoretical and experimental investigations find that the NS arrays are effective in harvesting light over a wide range of the λ and the incident angle, showing their broadband and omnidirectional characteristics. The presented concept and the manufacturing technique for the light-harvesting NSs represent a viable, promising path toward high-efficiency solar cells and should benefit many other types of optoelectronic devices.

Acknowledgment

This work was supported by National Science Council of Taiwan (102-2628-M-002-006-MY3 and 101-2221-E-002-115-MY2) and National Taiwan University (103R7823).

References

[1] K.Q. Peng, S.T. Lee, Adv. Mater. 23 (2011) 198–215.
[2] A. Luque, S. Hegedus, Handbook of Photovoltaic Science and Engineering, Wiley, Chichester, 2003.
[3] J. Zhao, A. Wang, P.P. Altermatt, S.R. Wenham, M.A. Green, Sol. Energy Mater. Sol. Cells 42 (1996) 87–99.
[4] P. Doshi, G.E. Jellison, A. Rohatgi, Appl. Opt. 36 (1997) 7826–7837.
[5] K.Q. Peng, X. Wang, L. Li, X.L. Wu, S.T. Lee, J. Am. Chem. Soc. 132 (2010) 6872–6873.
[6] H.P. Wang, T.Y. Lin, C.W. Hsu, M.L. Tsai, C.H. Huang, W.R. Wei, M.Y. Huang, Y.J. Chien, P.C. Yang, C.W. Liu, L.J. Chou, J.H. He, ACS Nano 7 (2013) 9325–9335.
[7] L.K. Yeh, K.Y. Lai, G.J. Lin, P.H. Fu, H.C. Chang, C.A. Lin, J.H. He, Adv. Energy Mater. 1 (2011) 506–510.
[8] H.P. Wang, K.Y. Lai, Y.R. Lin, C.A. Lin, J.H. He, Langmuir 26 (2010) 12855–12858.

[9] J.Y. Jung, Z. Guo, S.W. Jee, H.D. Um, K.T. Park, M.S. Hyun, J.M. Yang, J.H. Lee, Nanotechnology 21 (2010) 445303–445309.
[10] B. Tian, T.J. Kempa, C.M. Lieber, Chem. Soc. Rev. 38 (2009) 16–24.
[11] E.C. Garnett, P.D. Yang, J. Am. Chem. Soc. 130 (2008) 9224-9225.
[12] E. Garnett, P.D. Yang, Nano Lett. 10 (2010) 1082–1087.
[13] D.M. Schaadt, B. Feng, E.T. Yu, Appl. Phys. Lett. 86 (2005) (063106-1-3).
[14] P.H. Fu, G.J. Lin, C.H. Ho, C.A. Lin, C.F. Kang, Y.L. Lai, K.Y. Lai, J.H. He, Appl. Phys. Lett. 100 (2012) (013105-1-4).
[15] C.F. Bohren, D.R. Huffman, Absorption and Scattering of Light by Small Particles, Wiley, New York, 1983.
[16] Z. Sun, X. Zuo, Y. Yang, Opt. Lett. 37 (2012) 641–643.
[17] K.R. Catchpole, A. Polman, Appl. Phys. Lett. 93 (2008) (191113-1-3).
[18] D. Derkacs, S.H. Lim, P. Matheu, W. Mar, E.T. Yu, Appl. Phys. Lett. 89 (2006) (093103-1-3).
[19] K.Q. Peng, X. Wang, X.L. Wu, S.T. Lee, Nano Lett. 9 (2009) 3704–3709.
[20] Y.A. Akimov, W.S. Koh, S.Y. Sian, S. Ren, Appl. Phys. Lett. 96 (2010) (073111-1-3).
[21] C.K. Huang, K.W. Sun, W.L. Chang, Opt. Express 20 (2012) A85–A93.
[22] H.C. Chang, K.Y. Lai, Y.A. Dai, H.H. Wang, C.A. Lin, J.H. He, Energy Environ. Sci. 4 (2011) 2863–2869.
[23] J. Cai, J. Ye, S. Chen, X. Zhao, D. Zhang, S. Chen, Y. Ma, S. Jin, L. Qi, Energy Environ. Sci. 5 (2012) 7575–7581.
[24] Y.C. Chao, C.Y. Chen, C.A. Lin, J.H. He, Energy Environ. Sci. 4 (2011) 3436–3441.
[25] H.P. Wang, K.T. Tsai, K.Y. Lai, T.C. Wei, Y.L. Wang, J.H. He, Opt. Express 20 (2012) A94–A103.
[26] X.D. Wang, C.S. Lao, E. Graugnard, C.J. Summers, Z.L. Wang, Nano Lett. 5 (2005) 1784–1788.
[27] L. Li, T.Y. Zhai, H.B. Zeng, X.S. Fang, Y. Bando, D. Golberg, J. Mater. Chem. 21 (2011) 40–56.
[28] Y.R. Lin, K.Y. Lai, H.P. Wang, J.H. He, Nanoscale 2 (2010) 2765–2768.
[29] H.C. Vandehulst, Astrophys. J. 112 (1950) 1–5.
[30] J.R. Meyer-Arendt, Introduction to Classical and Modern Optics, Prentice Hall, New Jersey, 1995.
[31] M. Kerker, The Scattering of Light and Other Electromagnetic Radiation, Academic Press, New York, 1969.
[32] L. Cao, J.S. White, J.S. Park, J.A. Schuller, B.M. Clemens, M.L. Brongersma, Nat. Mater. 8 (2009) 643–647.
[33] L. Cao, P. Fan, A.P. Vasudev, J.S. White, Z. Yu, W. Cai, J.A. Schuller, S. Fan, M.L. Brongersma, Nano Lett. 10 (2010) 439–445.
[34] O. Isabella, J. Krc, M. Zeman, Appl. Phys. Lett. 97 (2010) (101106-1-3).
[35] M.D. Kelzenberg, S.W. Boettcher, J.A. Petykiewicz, D.B. Turner-Evans, M.C. Putnam, E.L. Warren, J.M. Spurgeon, R.M. Briggs, N.S. Lewis, H.A. Atwater, Nat. Mater. 9 (2010) 239–244.
[36] J.Y. Lee, P. Peumans, Opt. Express 18 (2010) 10078–10087.
[37] H.C. Liao, C.S. Tsao, T.H. Lin, M.H. Jao, C.M. Chuang, S.Y. Chang, Y.C. Huang, Y.T. Shao, C.Y. Chen, C.J. Su, U. S. Jeng, Y.F. Chen, W.F. Su, Acs Nano 6 (2012) 1657–1666.
[38] S. Das, A. Kundu, H. Saha, S.K. Datta, J. Mod. Opt. 59 (2012) 1219–1231.
[39] C.-Y. Fang, Y.-L. Liu, Y.-C. Lee, H.-L. Chen, D.-H. Wan, C.-C. Yu, Adv. Funct. Mater. 23 (2013) 1412–1421.
[40] X.Y. Ma, J.Q. Lu, R.S. Brock, K.M. Jacobs, P. Yang, X.H. Hu, Phys. Med. Biol. 48 (2003) 4165–4172.
[41] R.A. Soref, B.R. Bennett, IEEE J. Quant. Electron QE-23 (1987) 123–129.
[42] J. Li, L. Xue, Z. Wang, Y. Han, Colloid Polym. Sci. 285 (2007) 1037–1041.
[43] J.P. Berenger, J. Comput. Phys. 114 (1994) 185–200.

Guan-Jhong Lin received his M.S. degrees in Photonics and Optoelectronics from National Taiwan University in 2012. His research focuses on the efficiency enhancement of nitride- and silicon-based optoelectronic devices.

Hsin-Ping Wang received her M.S. degree (2011) in the Graduate Institute of Photonics and Optoelectronics at National Taiwan University, Taipei, Taiwan. She is now a Ph. D. student in Dr. Jr-Hau He's group and currently works in UCSD and UC Berkeley as a visiting scholar. Her research interests include theoretical and experimental research on optical properties analysis of nanostructure, varied types of solar cells (including conventional Si solar cell, thin-film solar cell, a-Si solar cell, and Si heterojunction solar cell), and solar water splitting cells.

Der-Hsien Lien received B.S. degree (2003) and the M.S. degree (2005) in the Department of Materials Science and Engineering from National Tsing Hua University, Hsinchu, Taiwan. He is a Ph.D. student in the Graduate Institute of Electronics Engineering at National Taiwan University, and currently works in the Electrical Engineering & Computer Sciences, UC Berkeley as a visiting scholar. His research interests include the dynamics and applications of nanophotonics, green memory devices, 2D materials physics and flexible optoelectronics.

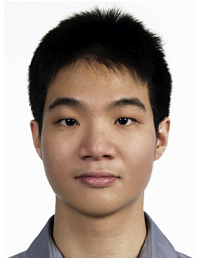

Po-Han Fu received his B.S. degree in 2010 and M.S degree in 2012 from National Taiwan University. He is currently a Ph.D. student of the institute of photonics and optoelectronics in National Taiwan University. His current research focuses on integrated silicon photonics.

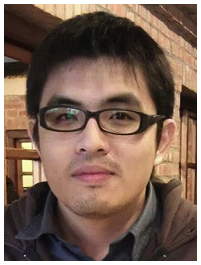

Hung-Chih Chang received the B.S. degree in engineering science and ocean engineering from the National Taiwan University, Taipei, Taiwan, in 2009 and the M.S. degree from Graduate Institute of Photonics and Optoelectronics, National Taiwan University, Taipei, Taiwan, in 2011. He is currently an advanced engineer with the R&D Department of Advanced Technology Development, Motech Industries, Inc. Science Park Branch. His primary research interests include nanowire, antireflection coating, photon management in silicon, and high efficiency industrial Si solar cells.

Cheng-Han Ho obtained the Bachelor degree from the Department of Electrophysics National Chiao Tung University in 2006. He received his Master degree in Graduate Institute of Photonics and Optoelectronics, National Taiwan University in 2012. In graduate school, his research focused on light emitting diodes and solar cells of InGaN/GaN materials. After one year military service, he currently is a research and development engineer in an equipment manufacturing company.

Chin-An Lin received the B.S degree in Physics from National Kaohsiung Normal University, Kaohsiung, Taiwan, in 2006. In 2007, he joined Dr. Jr-Hau He's group in Graduate Institute of Photonics and Optoelectronics, National Taiwan University, Taipei, Taiwan, and received his M.S. degree in 2008. He now is Dr. Jr-Hau He's Ph. D. student and his current research interests include the antireflective coatings in solar cells and the dye-sensitized solar cell.

Kun-Yu Lai is currently an assistant professor in the Department of Optics and Photonics at National Central University (NCU) in Taiwan. Dr. Lai received his Ph.D. degree in Electrical Engineering from North Carolina State University in 2009. After working as the postdoctoral fellow in the Graduate Institute of Photonics and Optoelectronics at National Taiwan University in 2009-2011, he joined the faculty in the Department of Optics and Photonics at NCU, where he specialized in the growth/fabrication of novel III-nitrides optoelectronic devices and the optical properties of low-dimensional structures, such as quantum wells, quantum dots, and nanowires.

Jr-Hau He received his B.S. and Ph.D. degrees from the National Tsing Hua University, Hsinchu, Taiwan, in 1999 and 2005, respectively. He is currently an Associate Professor at the Institute of Photonics and Optoelectronics and the Department of Electrical Engineering, National Taiwan University, Taipei, Taiwan. He is involved in the design of new nanostructured architectures for nanophotonics and the next generation of nanodevices, including photovoltaics, and resistive memory. Prof. He is a recipient of the Outstanding Young Electrical Engineer Award from the Chinese Institute of Electrical Engineering (2013), the Outstanding Youth Award of the Taiwan Association for Coating and Thin Film Technology (2012), the Youth Optical Engineering Medal of the Taiwan Photonics Society (2011), and has won numerous other awards and honors with his students in professional societies and conferences internationally.